

An Amphiphilic Pillar[5]arene: Synthesis, Controllable Self-Assembly in Water, and Application in Calcein Release and TNT Adsorption

Yong Yao, Min Xue, Jianzhuang Chen, Mingming Zhang, and Feihe Huang^{*}

MOE Key Laboratory of Macromolecular Synthesis and Functionalization, Department of Chemistry, Zhejiang University, Hangzhou 310027, P. R. China;

Email: fhuang@zju.edu.cn;

Supporting Information (21 pages)

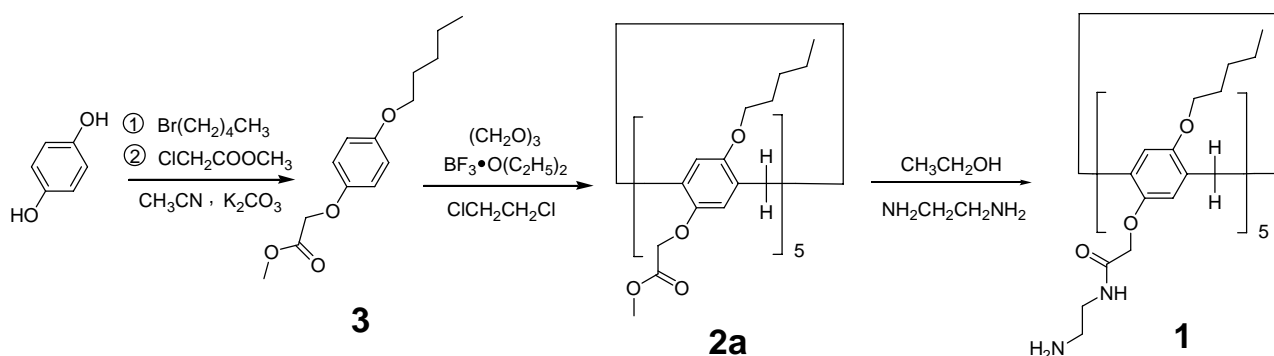
1.	<i>Materials and methods</i>	S2
2.	<i>Synthesis of the amphiphilic pillar[5]arene 1</i>	S3
3.	<i>Synthesis of the monomeric analog 4</i>	S11
4.	<i>The study of the transformation from vesicles to micelles</i>	S13
5.	<i>UV-vis study of the aggregation process</i>	S16
6.	<i>AFM, TEM and SEM studies of the microfibers</i>	S16
7.	<i>The mechanism of the self-assembly process</i>	S18
8.	<i>Application of the microtubes of 1 in the adsorption of TNT</i>	S20
9.	<i>Another advantage of macrocyclic amphiphiles</i>	S21

1. Materials and methods

Hydroquinone, methyl chloroacetate, bromopentane, boron trifluoride diethyl etherate, ethanediamine, 1,2-dichloroethane were reagent grade and used as received. Solvents were either employed as purchased or dried according to procedures described in the literature. ^1H NMR and ^{13}C NMR spectra were recorded on a Bruker Avance DMX-400 spectrometer. Mass spectra were obtained on a Bruker Esquire 3000 plus mass spectrometer (Bruker-Franzen Analytik GmbH Bremen, Germany) equipped with an ESI interface and an ion trap analyzer. HRMS were obtained on a WATERS GCT Premier mass spectrometer. UV-vis spectra were taken on a Perkin-Elmer Lambda 35 UV-vis spectrophotometer. FT-IR spectra were taken with potassium bromide pellets on a TENSOR 27 spectrometer. The melting points were collected on a SHPSIC WRS-2 automatic melting point apparatus. FE-SEM was applied to investigate the morphology, which was carried out with a Hitachi S-4800 field emission scanning electron microscope. TEM images were obtained using a Philips TECNAI-12 instrument with an accelerating voltage of 120 kV. AFM images were obtained using a Multi-Mode Nanoscope-IIIa Scanning Probe Microscope (Veeco Company, USA) in the tapping mode. Dynamic light scattering measurements were performed on a goniometer ALV/CGS-3 using a UNIPHASE He-Ne laser operating at 632.8 nm.

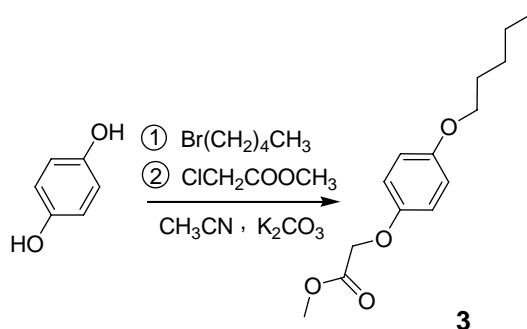
2. Synthesis of the amphiphilic pillar[5]arene **1**

Scheme S1. Synthetic route for compound **1**



2.1. Synthesis of monomer **3**

Scheme S2. Synthesis of compound **3**



Anhydrous potassium carbonate (55.2 g, 400 mmol) was added to a solution of hydroquinone (44.0 g, 400 mmol) and bromopentane (60.5 g, 400 mmol) in dry acetonitrile (500 mL) under vigorous stirring. The mixture was stirred at 80 °C for 24 hours under nitrogen atmosphere.^{S1} Then methyl chloroacetate (43.2 g, 400 mmol) and additional anhydrous potassium carbonate (55.2 g, 400 mmol) were added into the reaction mixture and reacted for another 24 hours. After removal of the inorganic salt, the solvent was evaporated and the residue was purified by chromatography on silica gel (petroleum ether/ethyl acetate, v/v 10:1) to give **3** as a white solid (47.0 g, 45%). Mp: 83.4–85.1 °C. The proton NMR spectrum of **3** is shown in Figure S1. ^1H NMR (400 MHz, chloroform-*d*, 293K) δ (ppm): 6.82 (m, 4H), 4.57 (s, 2H), 3.88 (t, $J = 6.0$ Hz, 2H), 3.78 (s, 3H), 1.78–1.71 (m, 2H), 1.43–1.36 (m, 4H), 0.92 (t, $J = 6.0$ Hz, 3H). The ^{13}C NMR spectrum of **3** is shown in Figure S2. ^{13}C NMR (100 MHz, chloroform-*d*, 293K) δ (ppm): 169.70, 154.16, 151.86, 115.82, 115.39, 68.53, 66.26, 52.16, 29.05, 28.21, 22.47, 14.03. LRESIMS is shown in Figure S3: m/z 275.2 [**3** + Na] $^+$ (100%), 291.1 [**3** + K] $^+$ (10%). HRESIMS: m/z calcd for [**3** + Na] $^+$ $\text{C}_{14}\text{H}_{20}\text{NaO}_4$, 275.1259; found, 275.1254; error –1.8 ppm.

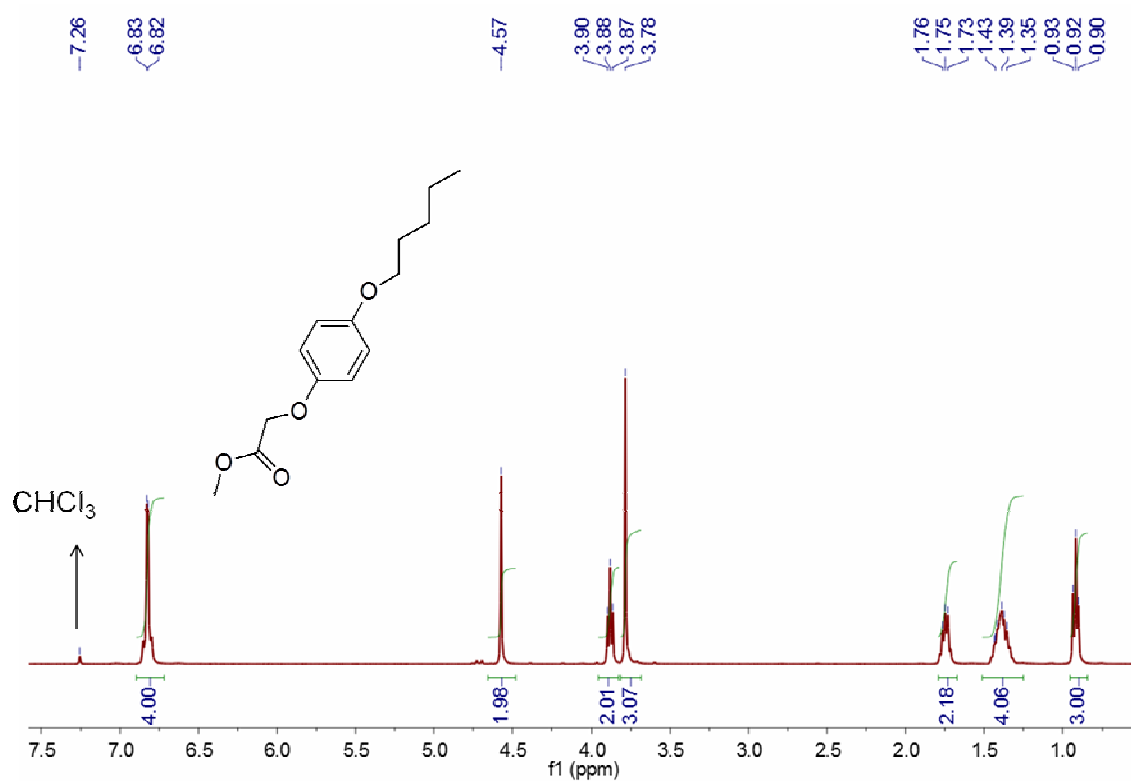


Figure S1. ^1H NMR spectrum (400 MHz, CDCl_3 , 293 K) of monomer **3**.

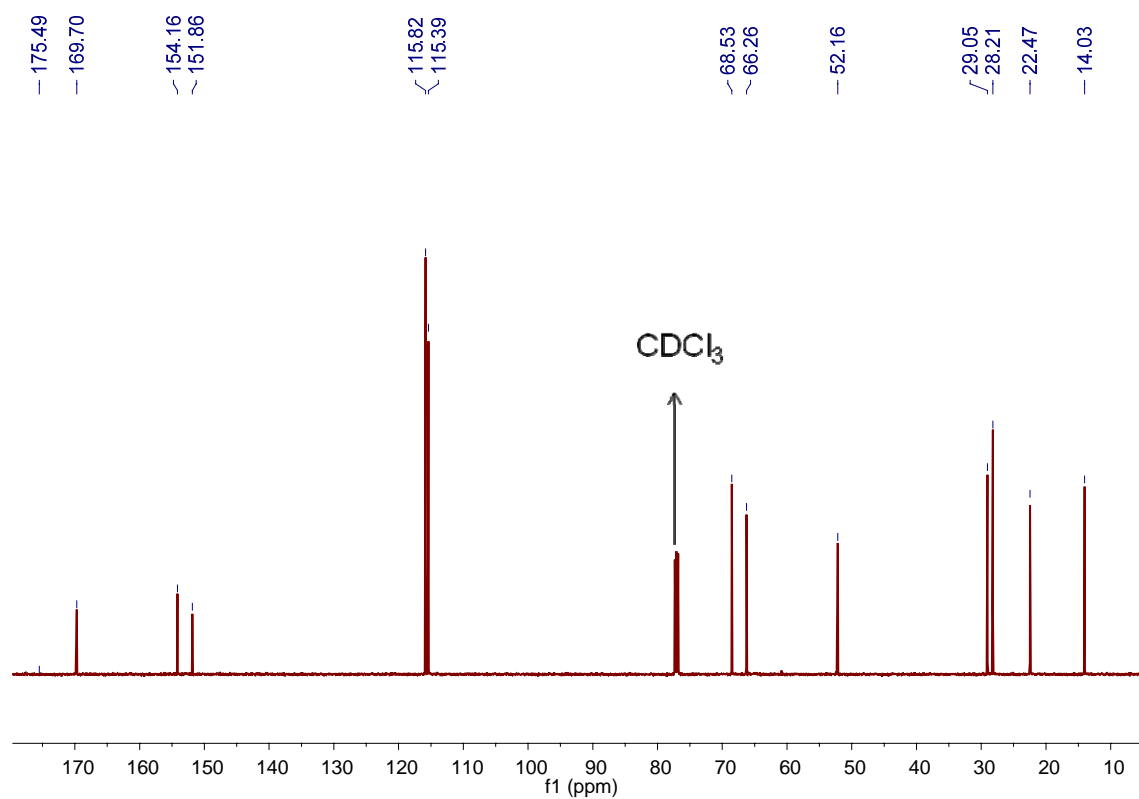


Figure S2. ^{13}C NMR spectrum (100 MHz, CDCl_3 , 293 K) of monomer **3**.

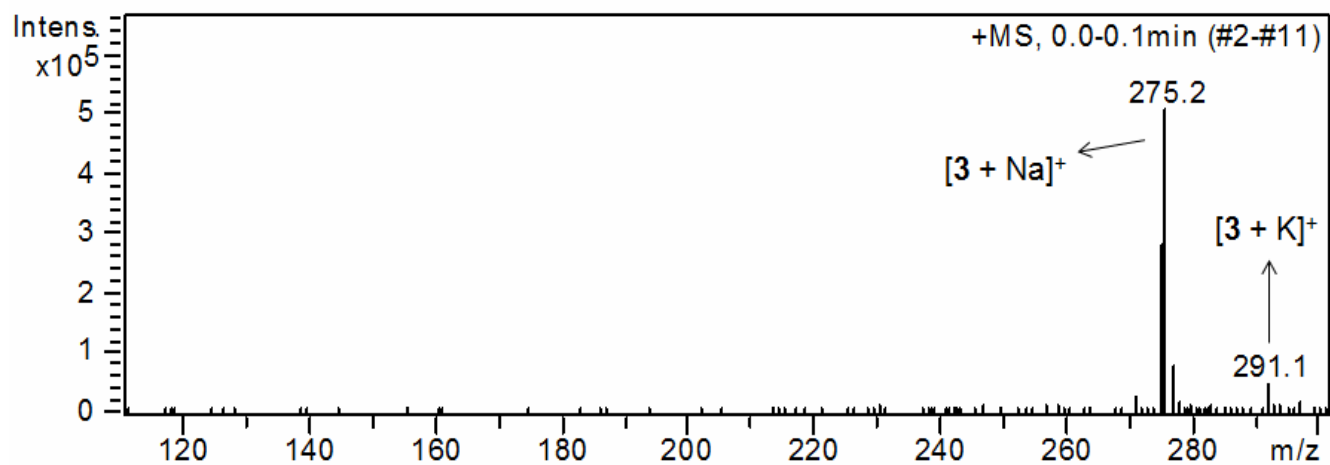
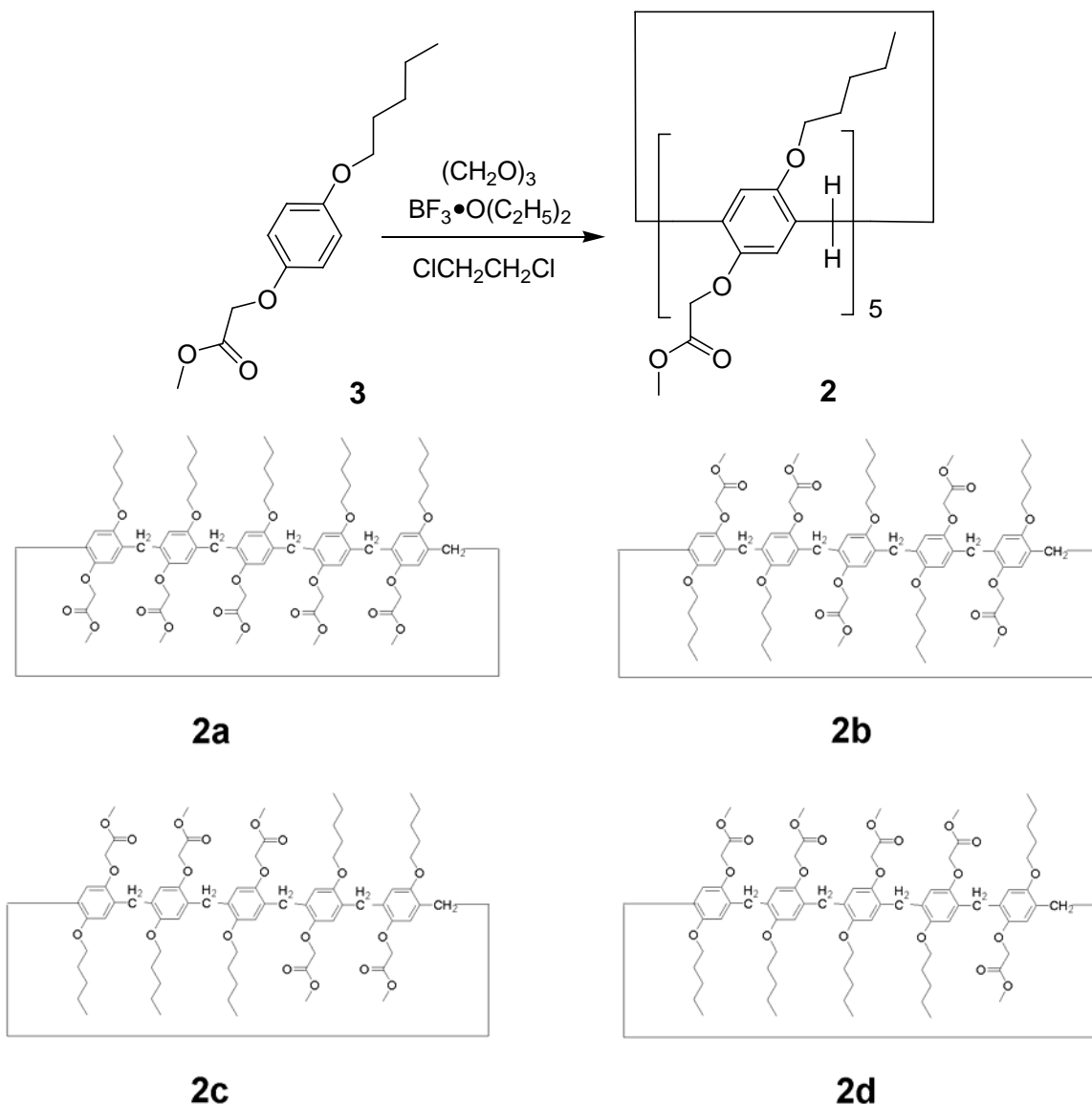


Figure S3. Electrospray ionization mass spectrum of monomer **3**. Assignment of main peaks: m/z 275.2 [**3** + Na]⁺ (100%) and 291.1 [**3** + K]⁺ (10%).

2.2. Synthesis of nonsymmetric pillar[5]arene **2a**

Scheme S3. Synthesis of compound **2a**



A solution of **3** (3.37 g, 11.5 mmol) and triformol (0.349 g, 11.5 mmol) in 1,2-dichloroethane (50 mL) was cooled with ice bath. Boron trifluoride etherate^{S2} (3.26 g, 23.0 mmol) was added to the solution and the mixture was stirred at room temperature for 1 hour. The reaction mixture was then washed by water (50 mL \times 2) and dried with Na_2SO_4 . The solvent was evaporated to provide a crude product, which was purified by column chromatography (eluent: petroleum ether/ethyl acetate, 5:1) to give a white solid **2** (0.80 g, 40%). Pillar[5]arene **2** has 4 constitutional isomers **2a**, **2b**, **2c**, and **2d**. Isomer **2a** had been recrystallized in a mixture of dichloromethane and methanol (v:v, 1:4) before it was used in the next step to make compound **1**. The proton NMR spectrum of **2a** (Mp: 102.1–102.9 °C) is shown in Figure S4. ^1H NMR (400 MHz, chloroform-*d*, 293K) δ (ppm): 7.05 (s, 5H), 6.79 (s, 5H), 4.57 (s, 10H), 3.89 (s, 10H), 3.82 (s, 10H), 3.48 (s, 15H), 1.88–1.81 (m, 10H), 1.60–1.52 (m, 10H), 1.45–1.37 (m, 10H), 0.97 (t, J = 4.0 Hz, 15H). The ^{13}C NMR spectrum of **2a** is shown in Figure S5. ^{13}C NMR (100 MHz, chloroform-*d*, 293K) δ (ppm): 170.03, 150.24, 148.39, 128.31, 128.23, 114.58, 114.31, 68.30, 65.47, 58.47,

51.73, 29.60, 29.30, 28.54, 22.64, 18.40, 14.06. LRESIMS is shown in Figure S6: m/z 1344.7 [**2a** + Na + H]⁺ (100%), 1360.1 [**2a** + K]⁺ (28%). HRESIMS: m/z calcd for [**2a** + Na]⁺ C₇₅H₁₀₀NaO₂₀, 1343.6706; found, 1343.6713; error 0.5 ppm.

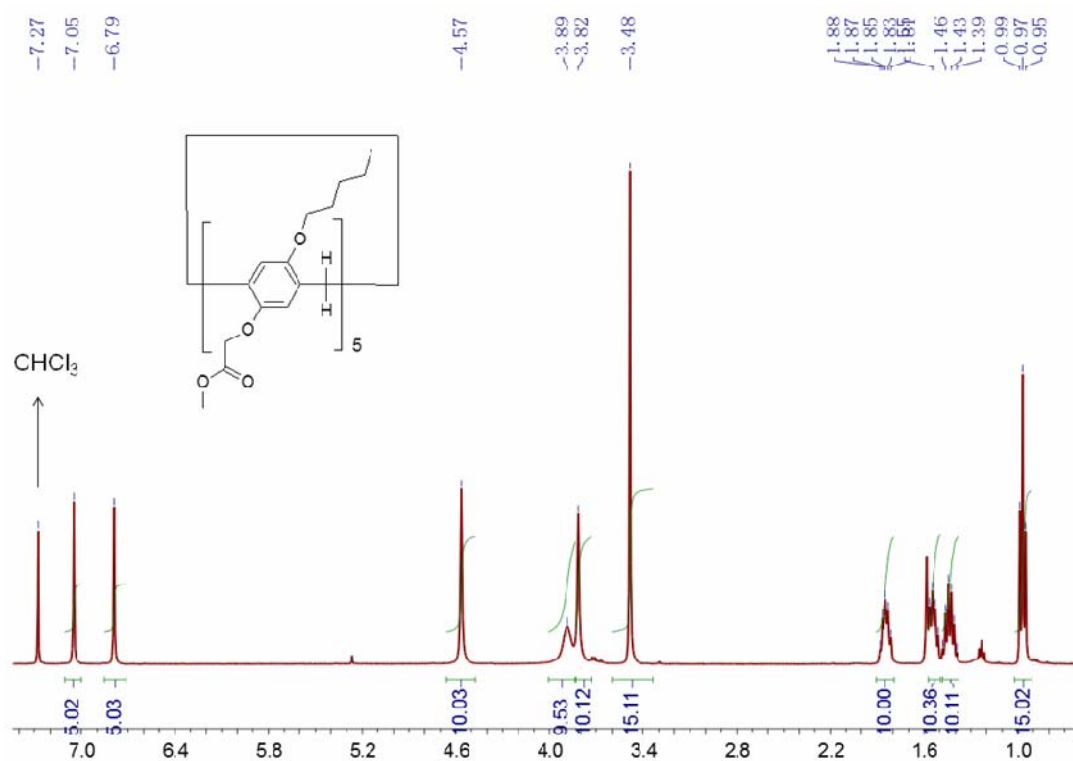


Figure S4. ¹H NMR spectrum (400 MHz, CDCl₃, 293 K) of pillar[5]arene **2a**.

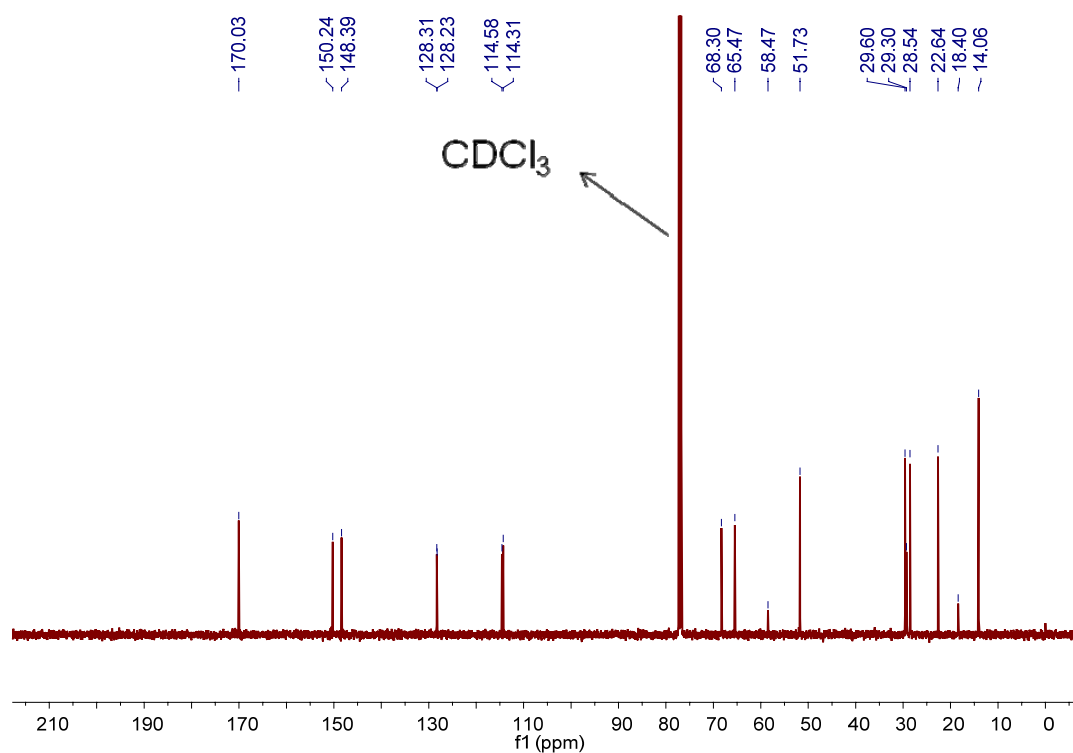


Figure S5. ¹³C NMR spectrum (100 MHz, CDCl₃, 293 K) of pillar[5]arene **2a**.

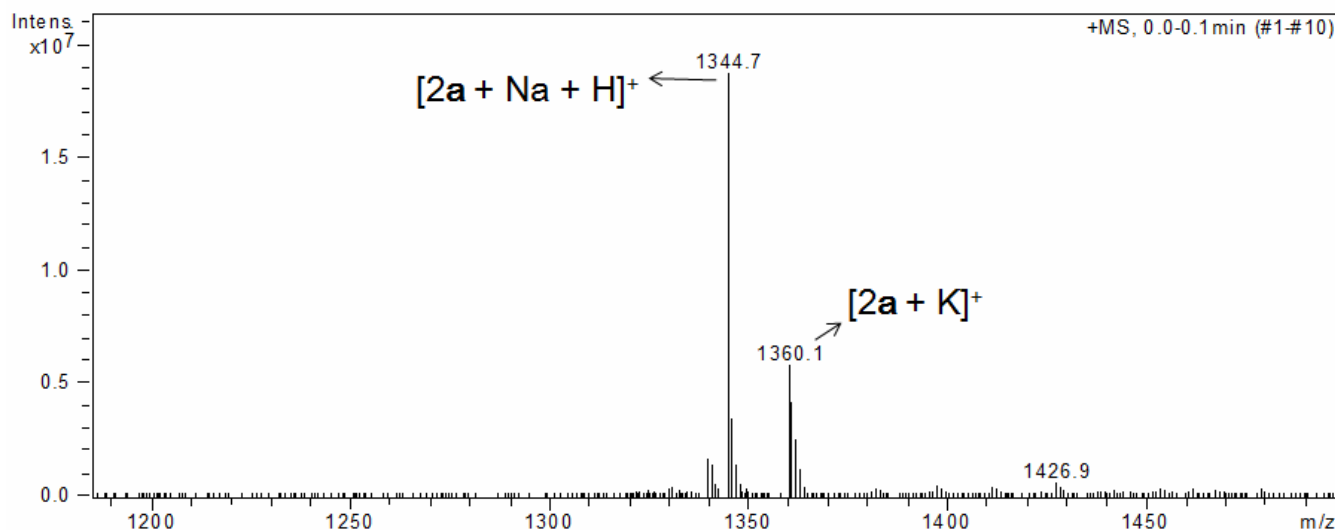


Figure S6. Electrospray ionization mass spectrum of pillar[5]arene **2a**. Assignment of main peaks: m/z 1344.7 [**2a** + Na + H]⁺ (100%) and 1360.1 [**2a** + K]⁺ (28%).

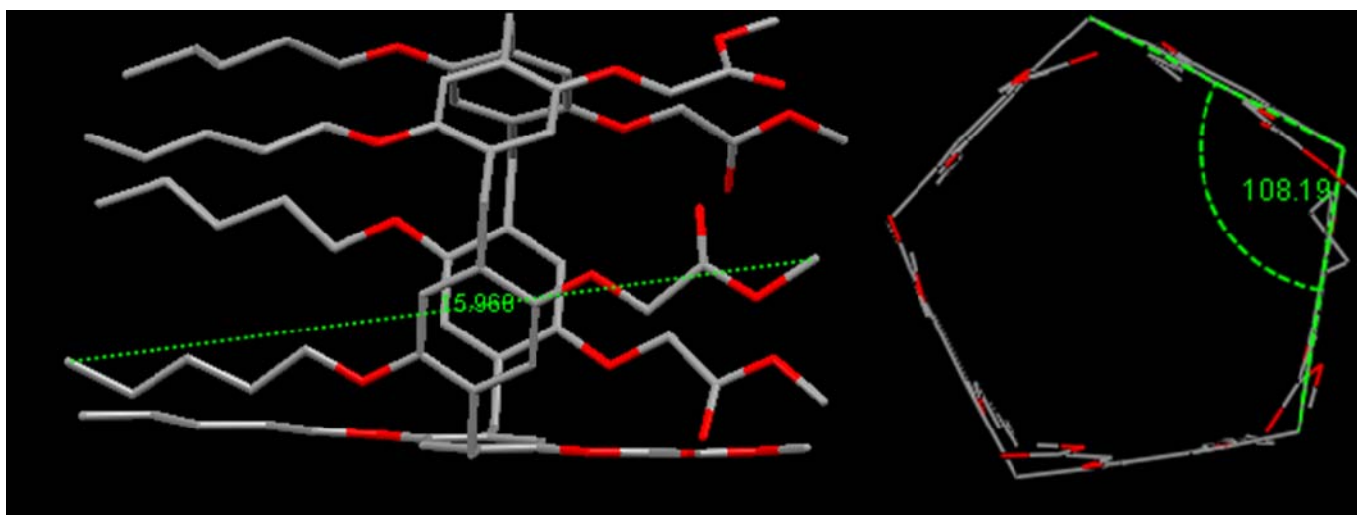


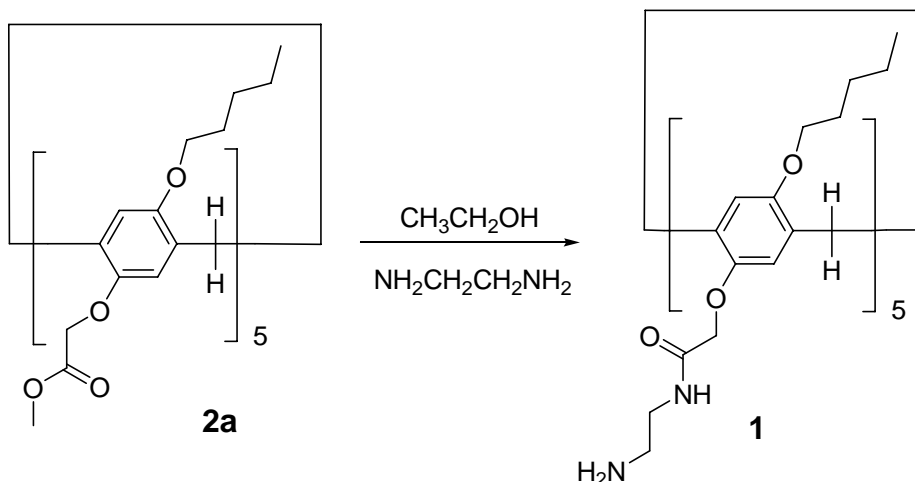
Figure S7. Crystal structure of the nonsymmetric pillar[5]arene **2a**. The unit for the distance is Å. The unit for the angle is degree. From this crystal structure, it is known that the extended molecular length of **2a** is about 1.6 nm. Since ethanediamine was introduced from **2a** to **1**, the extended molecular length of **1** is about 2 nm.

X-ray crystal data for 2a

Crystallographic data: block, colorless, $0.32 \times 0.26 \times 0.23$ mm³, C₇₅H₁₀₀O₂₀, *FW* 1321.55, monoclinic, space group *P* 2₁/*n*, $a = 21.5208(8)$, $b = 19.0796(5)$, $c = 22.3223(8)$ Å, $\alpha = 90^\circ$, $\beta = 114.517(4)^\circ$, $\gamma = 90^\circ$, $V = 8339.3(5)$ Å³, $Z = 4$, $D_c = 1.053$ g cm⁻³, $T = 293$ (2) K, $\mu = 0.618$ mm⁻¹, 29880 measured reflections, 14165 independent reflections, 866 parameters, 0 restraints, $F(000) = 2840$, $R(\text{int}) = 0.0356$, $R_1 = 0.0830$, $wR_1 = 0.1935$ (all data), $R_2 = 0.0629$, $wR_2 = 0.1755$ [$I > 2\sigma(I)$], max. residual density 0.902 e⁻Å⁻³, and goodness-of-fit (F^2) = 1.058.

2.3. Synthesis of amphiphilic pillar[5]arene **1**

Scheme S4. Synthesis of compound **1**



A mixture of **2a** (1.43 g, 1.00 mmol) and ethanediamine (5 mL) in ethanol (25 mL) was stirred in a 100 mL round-bottom flask at 90 °C for 24 hours. After cooling, the solvent was removed and the residue was poured into saturated brine (50 mL) to give a white solid (0.82 g, 53%). Mp: 202.3–204.5 °C. The proton NMR spectrum of **1** is shown in Figure S8. ^1H NMR (400 MHz, $\text{DMSO}-d_6$, 293 K) δ (ppm): 7.08 (s, 5H), 6.81 (s, 5H), 4.62–4.43 (m, 20H), 3.80–3.68 (m, 30H), 2.08 (m, 15H), 1.77 (s, 10H), 1.47–1.43 (m, 10H), 1.38–1.34 (m, 10H), 0.91 (t, $J = 4$ Hz, 15H). The ^{13}C NMR spectrum of **1** is shown in Figure S9. ^{13}C NMR (100 MHz, $\text{DMSO}-d_6$, 293 K) δ (ppm): 169.39, 149.47, 147.79, 127.64, 113.87, 67.81, 64.83, 51.51, 51.32, 28.99, 28.61, 27.92, 27.78, 22.08, 21.92, 13.77. LRESIMS is shown in Figure S10: m/z 1544.3 [**1** + CH_2Cl_2] $^-$ (100%). HRESIMS: m/z calcd for [**1** + Na] $^+$ $\text{C}_{80}\text{H}_{120}\text{N}_{10}\text{NaO}_{15}$, 1483.8832; found, 1483.8887; error 3.4 ppm.

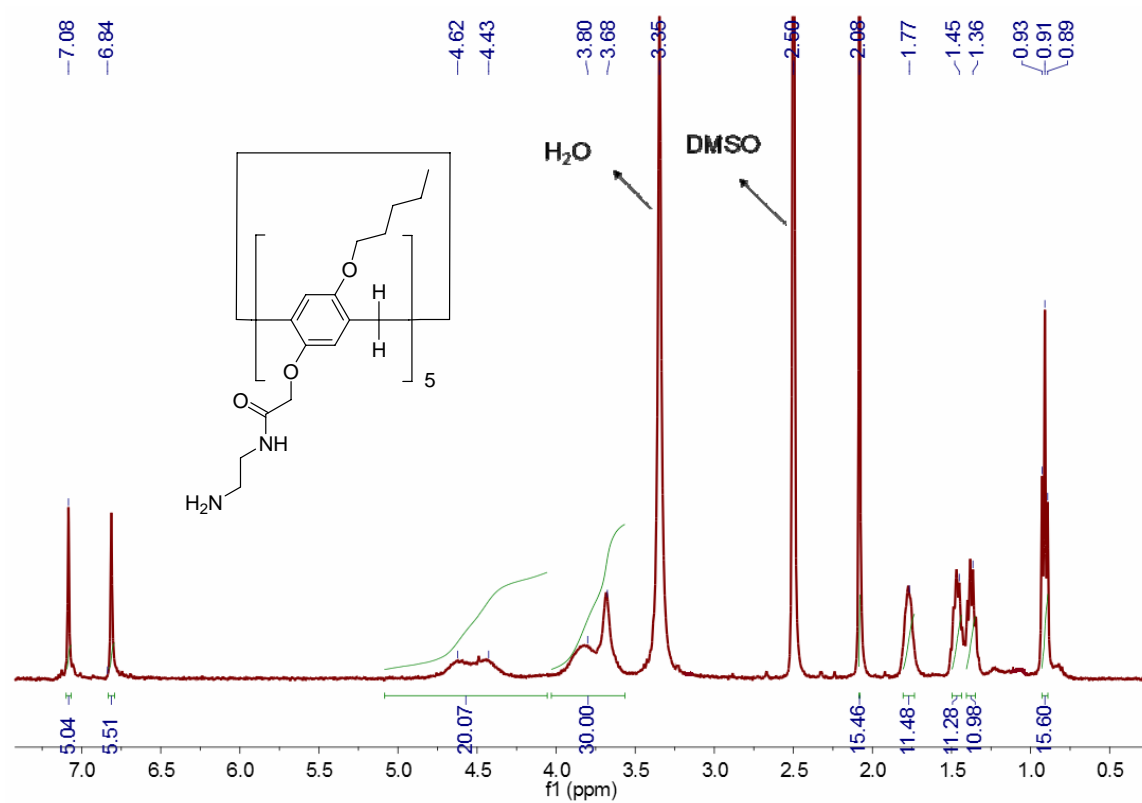


Figure S8. ^1H NMR spectrum (400 MHz, $\text{DMSO}-d_6$, 293 K) of the amphiphilic pillar[5]arene **1**.

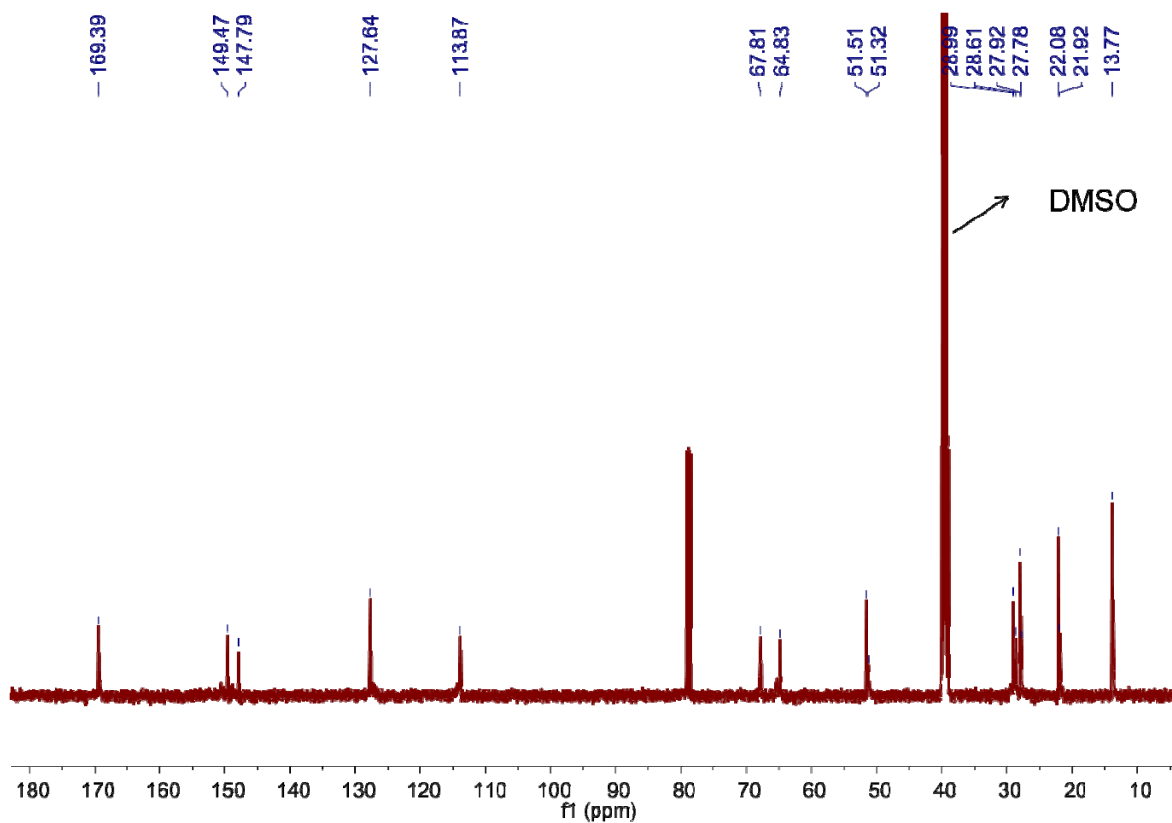


Figure S9. ^{13}C NMR spectrum (100 MHz, $\text{DMSO}-d_6$, 293 K) of the amphiphilic pillar[5]arene **1**.

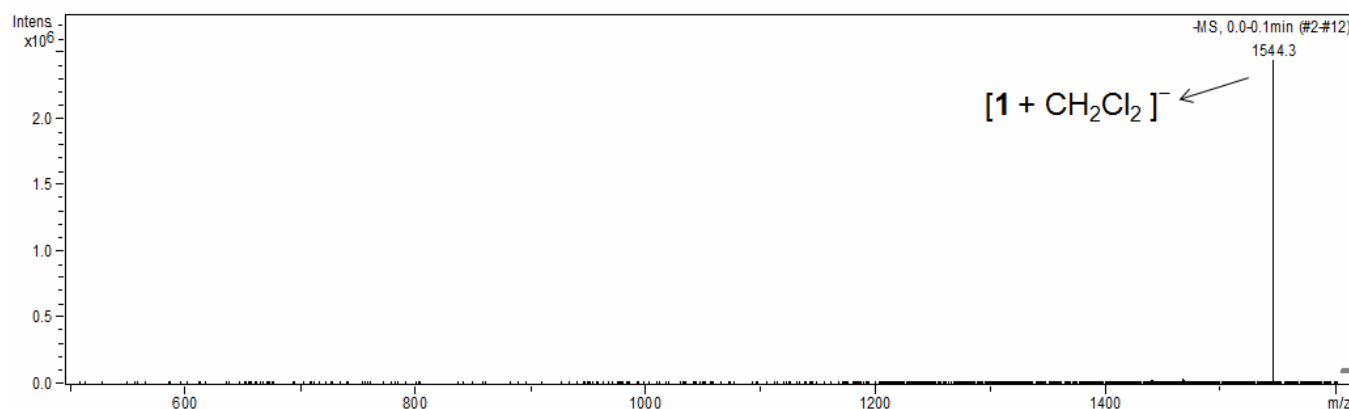
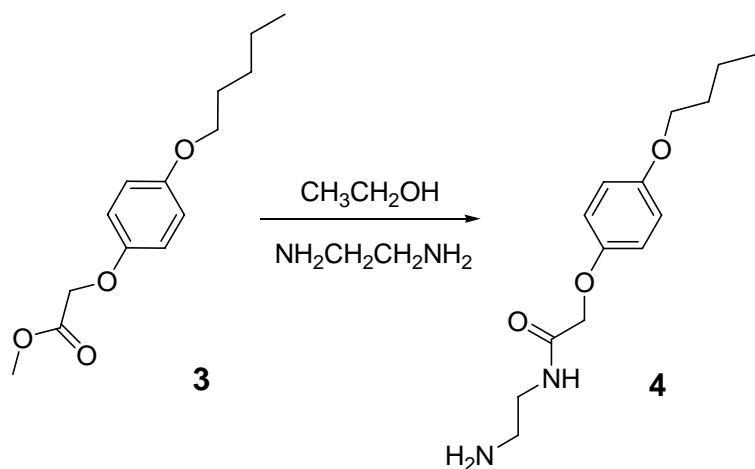


Figure S10. Electrospray ionization mass spectrum of the amphiphilic pillar[5]arene **1**. Assignment of the main peak: m/z 1544.3 $[1 + \text{CH}_2\text{Cl}_2]^-$ (100%). This peak is reasonable. First, precursor **2a** had been recrystallized in a mixture of dichloromethane and methanol (v:v, 1:4) before it was used in the preparation of amphiphilic pillar[5]arene **1**. Second, it was previously observed that a dichloromethane molecule could be included in the pillar[5]arene cavity in the solid state.^{7c,d}

3. Synthesis of the monomeric analog **4**

Scheme S5. Synthesis of compound **4**



A mixture of **3** (1.43 g, 5.00 mmol) and ethanediamine (5 mL) in ethanol (25 mL) was stirred in a 100 mL round-bottom flask at 90 °C for 24 hours. After cooling, the solvent was removed and the residue was poured into saturated brine (50 mL) to give a white solid (0.93 g, 60%). Mp: 188.3–190.1 °C. The ^1H NMR spectrum of **1** is shown in Figure S11. ^1H NMR (400 MHz, $\text{DMSO}-d_6$, 293 K) δ (ppm): 6.82 (s, 4H), 4.68 (s, 2H), 4.44 (s, 1H), 3.85 (t, J = 6.0 Hz, 2H), 3.67 (s, 4H), 3.40–3.36 (m, 2H), 1.66 (s, 2H), 1.33 (m, 4H), 0.87 (t, J = 6.0 Hz, 3H). The ^{13}C NMR spectrum of **1** is shown in Figure S12. ^{13}C NMR (100 MHz, $\text{DMSO}-d_6$, 293 K) δ (ppm): 169.78, 153.60, 151.87, 115.76, 115.49, 68.11, 65.49, 63.18, 52.02, 28.84, 28.10, 22.28, 14.12. LRESIMS is shown in Figure S13: m/z 280.2 $[\mathbf{4}]^+$ (100%). HRESIMS: m/z calcd for $[\mathbf{4} + \text{H}]^+$ $\text{C}_{15}\text{H}_{25}\text{N}_2\text{O}_3$, 281.1865; found 281.1865; error 0 ppm.

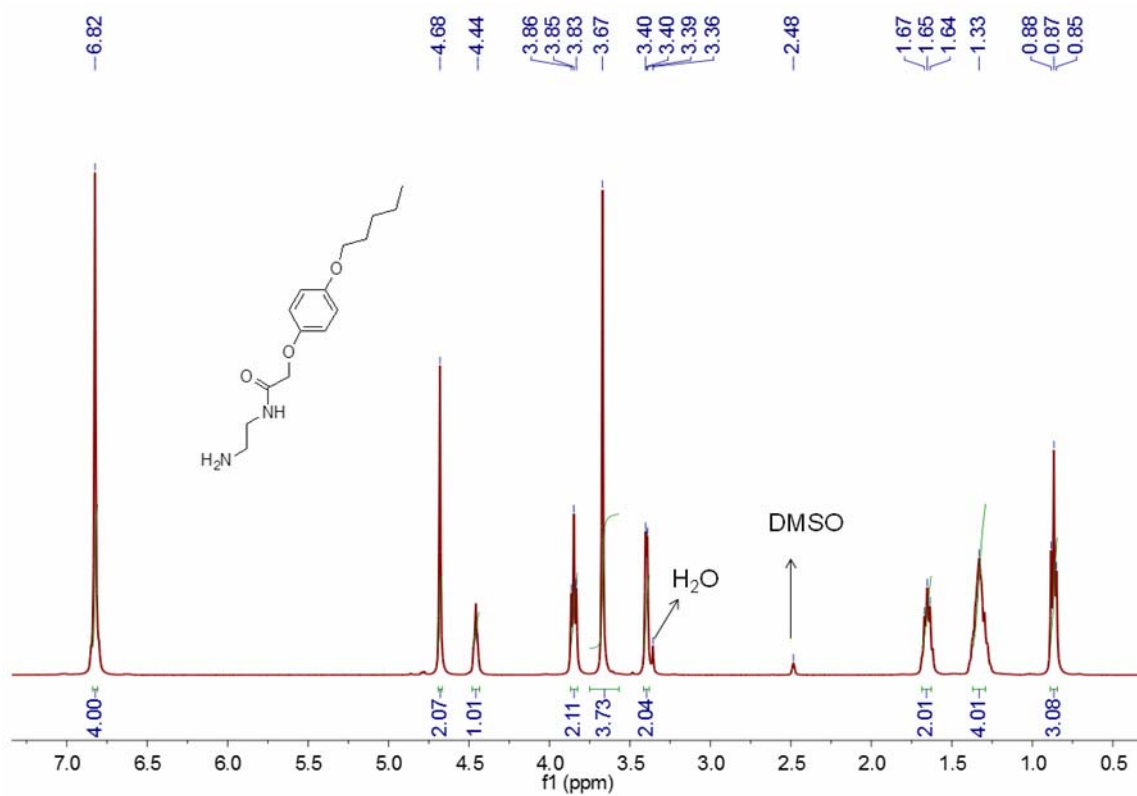


Figure S11. ¹H NMR spectrum (400 MHz, DMSO-*d*₆, 293 K) of the monomeric analog **4**.

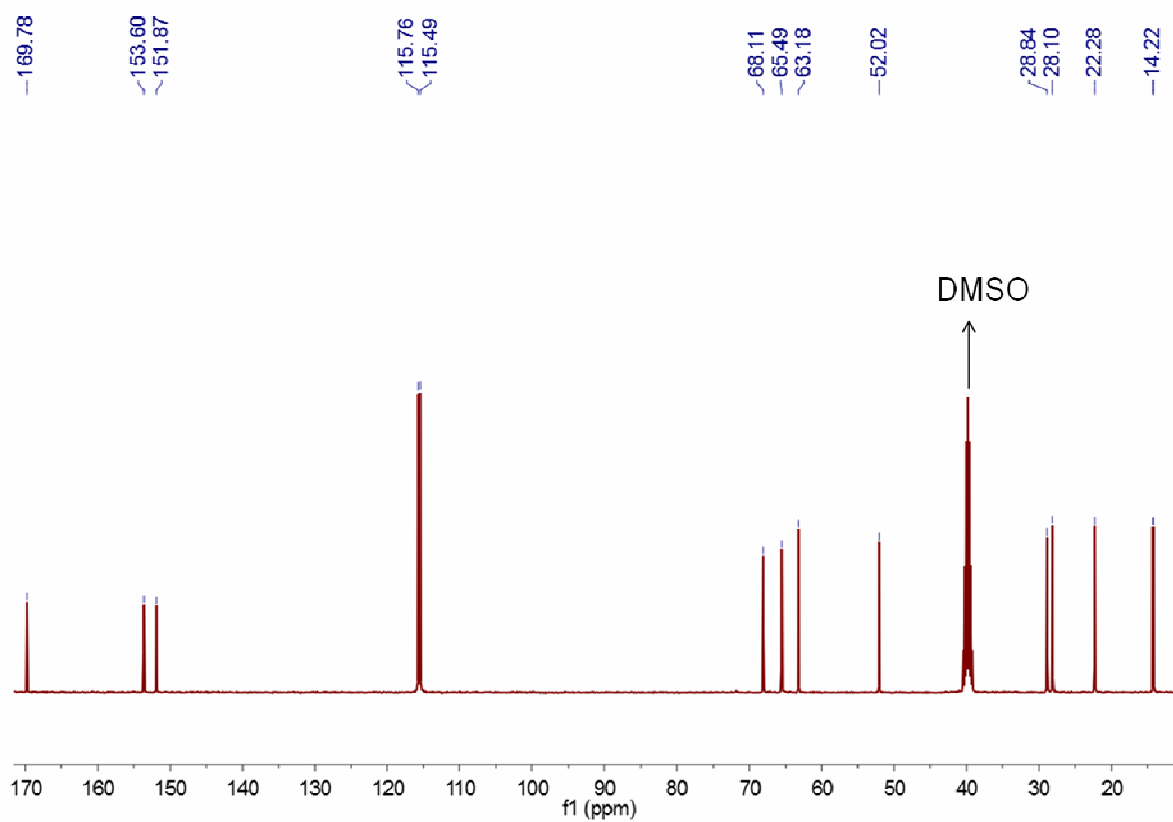


Figure S12. ¹³C NMR spectrum (100 MHz, DMSO-*d*₆, 293 K) of the monomeric analog **4**.

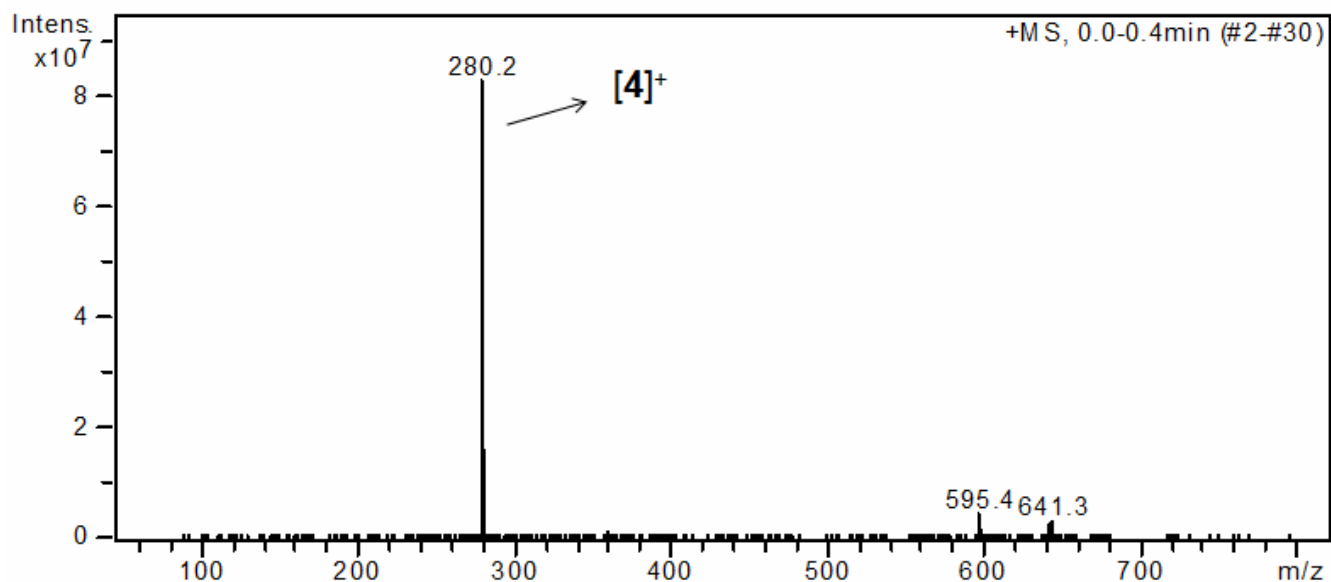


Figure S13. Electrospray ionization mass spectrum of the monomeric analog **4**. Assignment of the main peak: m/z 280.2 $[4]^+$ (100%).

4. The study of the transformation from vesicles to micelles

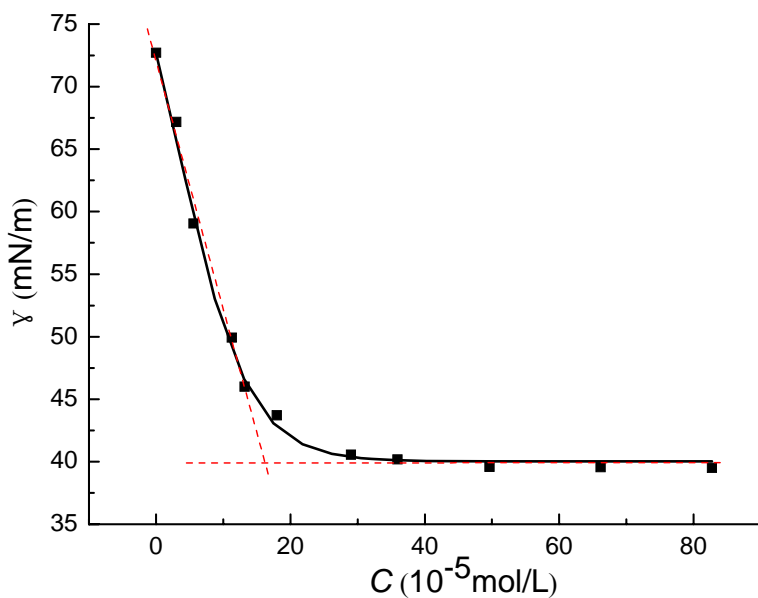


Figure S14. Surface tension of water as a function of the amphiphilic pillar[5]arene **1** concentration. There are two linear segments in the curve and a sudden reduction of the slope, implying that the CMC of **1** is approximately 1.5×10^{-4} M in water.

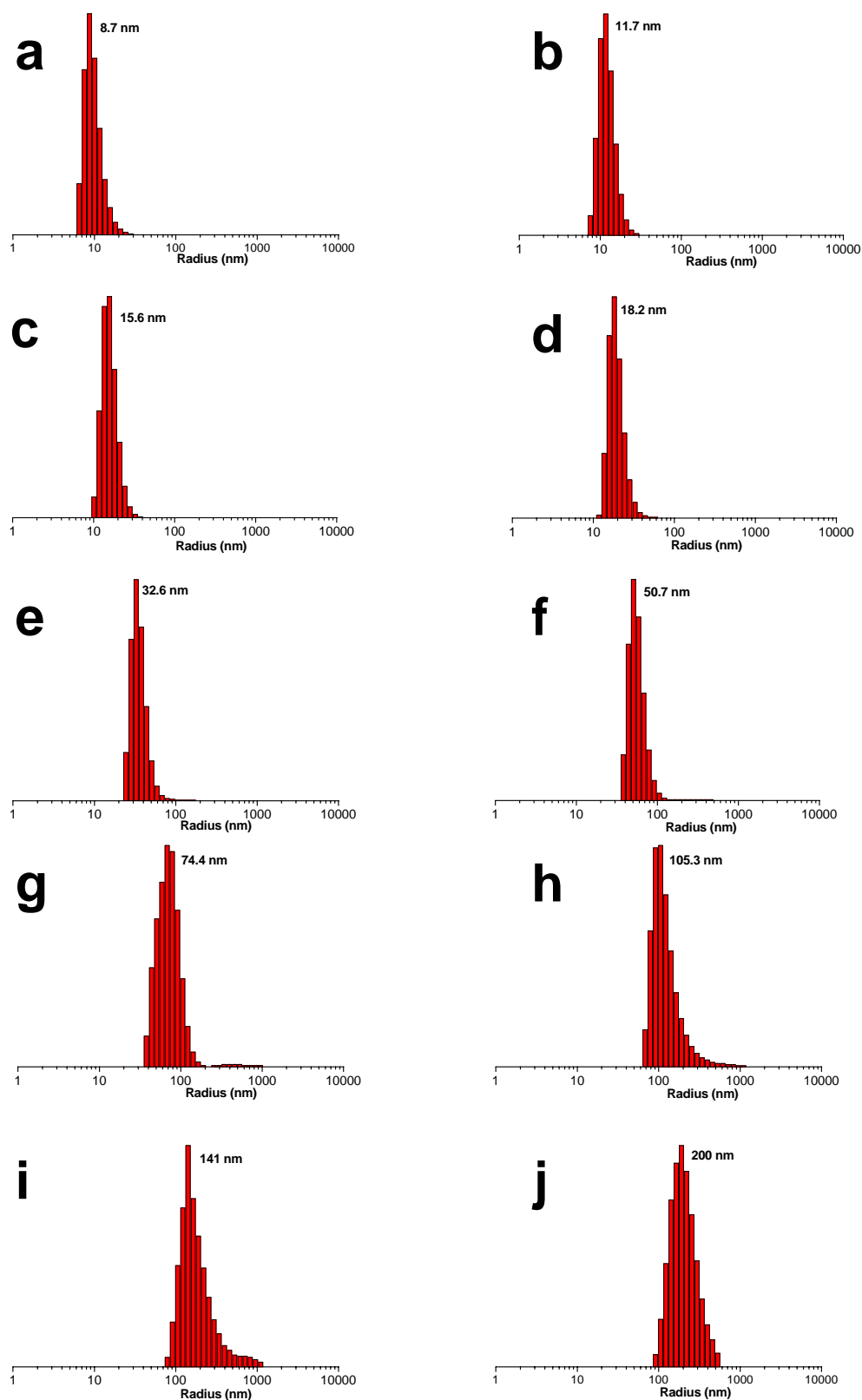


Figure S15. DLS results obtained from a solution of **1** (0.200 mM) as a function of pH at scattering angle of 90°: (a) pH = 3.0; (b) pH = 3.3; (c) pH = 3.6; (d) pH = 4.0; (e) pH = 4.5; (f) pH = 5.0; (g) pH = 5.5; (h) pH = 6.0; (i) pH = 6.5; (j) pH = 7.0.

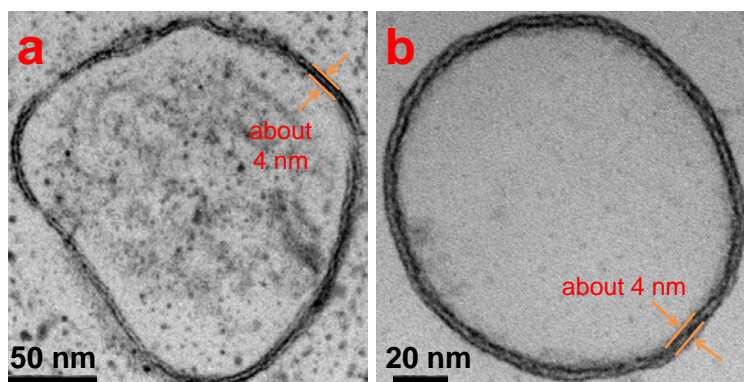


Figure S16. TEM images of vesicles after staining: (a) scalar bar is 50 nm; (b) scalar bar is 20 nm. One drop of a sample solution (2.00×10^{-4} M) was placed on a copper grid, put in a refrigerator for 1 h, and freeze-dried at -20 °C under reduced pressure. The specimens were subsequently post-fixed with 1% osmium tetroxide.

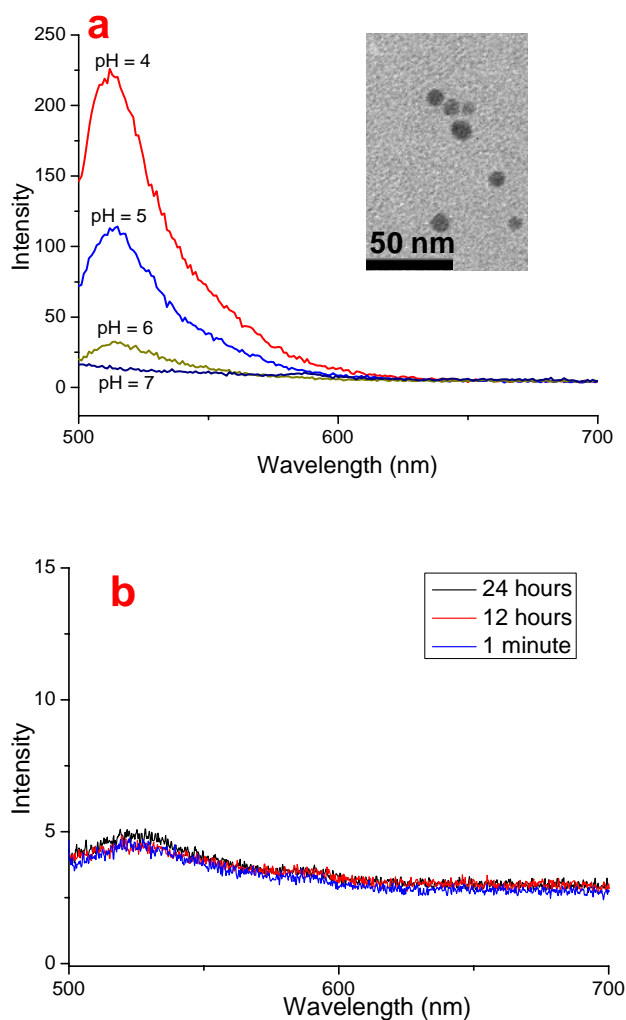


Figure S17. (a) Fluorescence emission spectra of calcein ($\lambda_{\text{exc}} = 525$ nm) encapsulated in a 2.0×10^{-4} M vesicular solution at different pH values. (b) Fluorescence emission spectra of calcein ($\lambda_{\text{exc}} = 525$ nm) encapsulated in a 2.0×10^{-4} M vesicular solution at different aging times when the pH was 7.^{S3} Please be noted that the scale increment of the vertical axis in (b) is much smaller than that in (a).

5. UV-vis study of the aggregation process

As shown in Figure S18a, after **1** was dissolved in water, the characteristic absorption peak of **1** at around 290 nm decreased with the aging time. This should be due to the decreasing concentration of **1** in the solution, which was caused by the formation of aggregates. The optical picture of the aggregates is shown in Figure S18b.

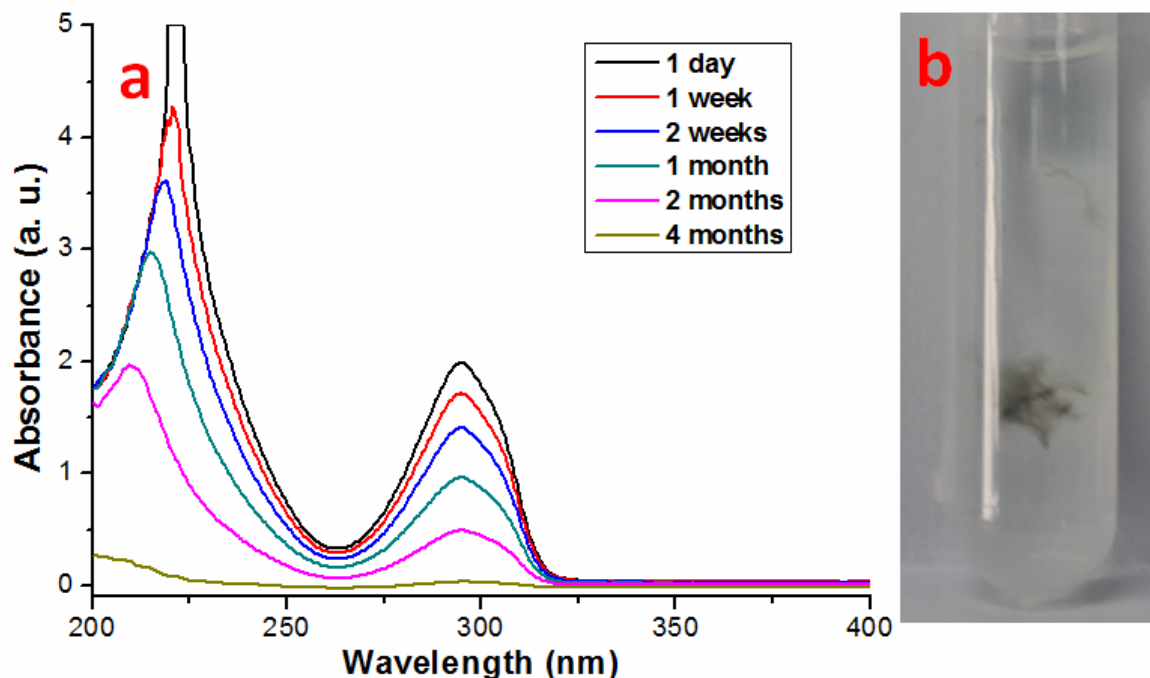


Figure S18. (a) UV-vis spectra of the amphiphilic pillar[5]arene **1** in water at different aging times; (b) the optical picture of the aggregates (15 days).

6. AFM, TEM and SEM studies of the microfibers.

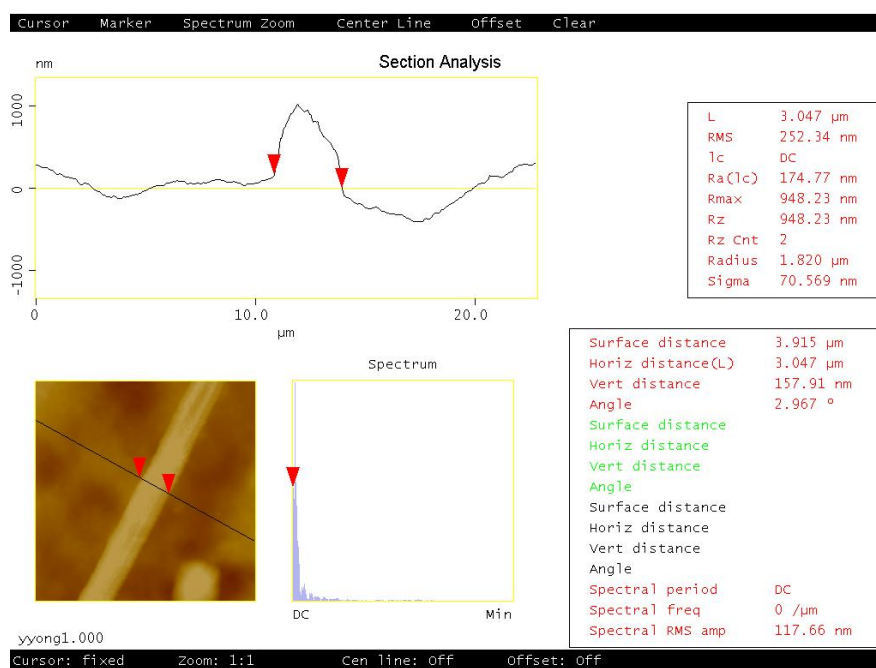


Figure S19. AFM image of a pillar[5]arene-based microfiber.

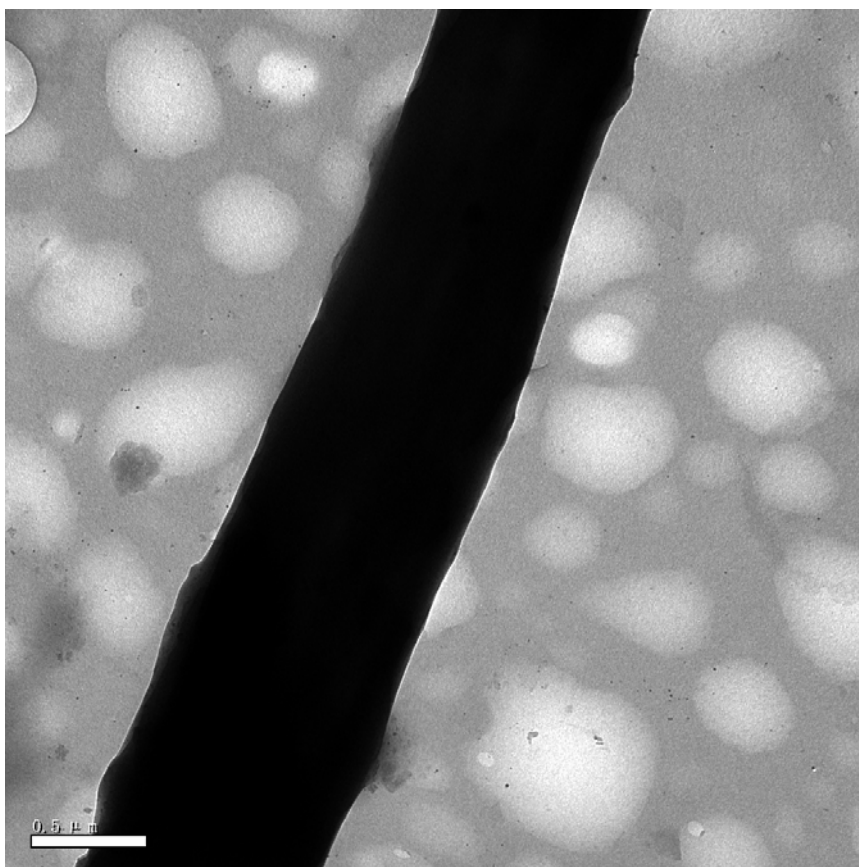


Figure S20. TEM image of a pillar[5]arene-based microfiber.

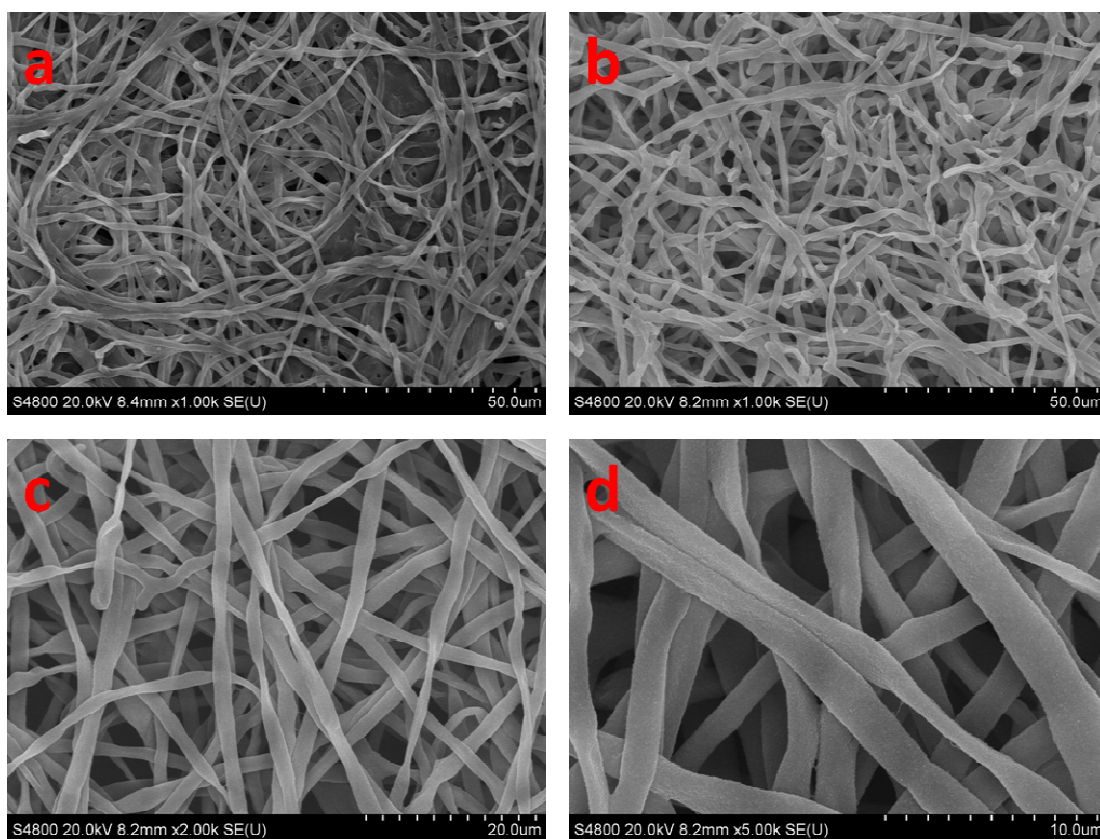


Figure S21. SEM images of the oblate microfibers.

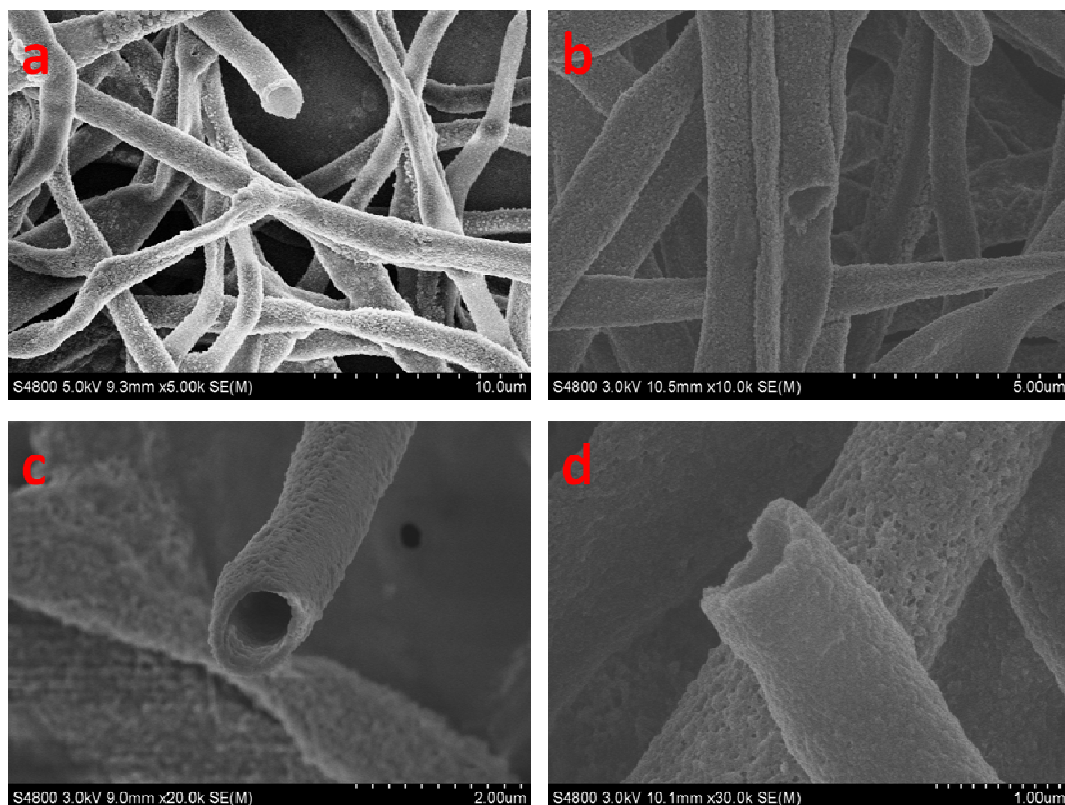


Figure S22. SEM images of the cross-sections of the microtubes: (a) scalar bar is 10 μm ; (b) scalar bar is 5 μm ; (c) scalar bar is 2 μm ; (d) scalar bar is 1 μm .

7. The mechanism of the self-assembly process

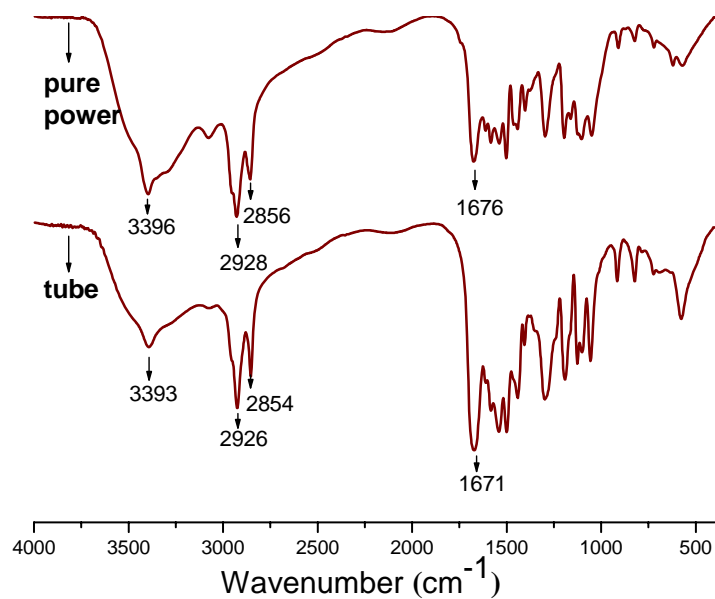


Figure S23. Comparison of the Fourier transform IR spectrum of a powder sample of **1** with that of the microtubes.

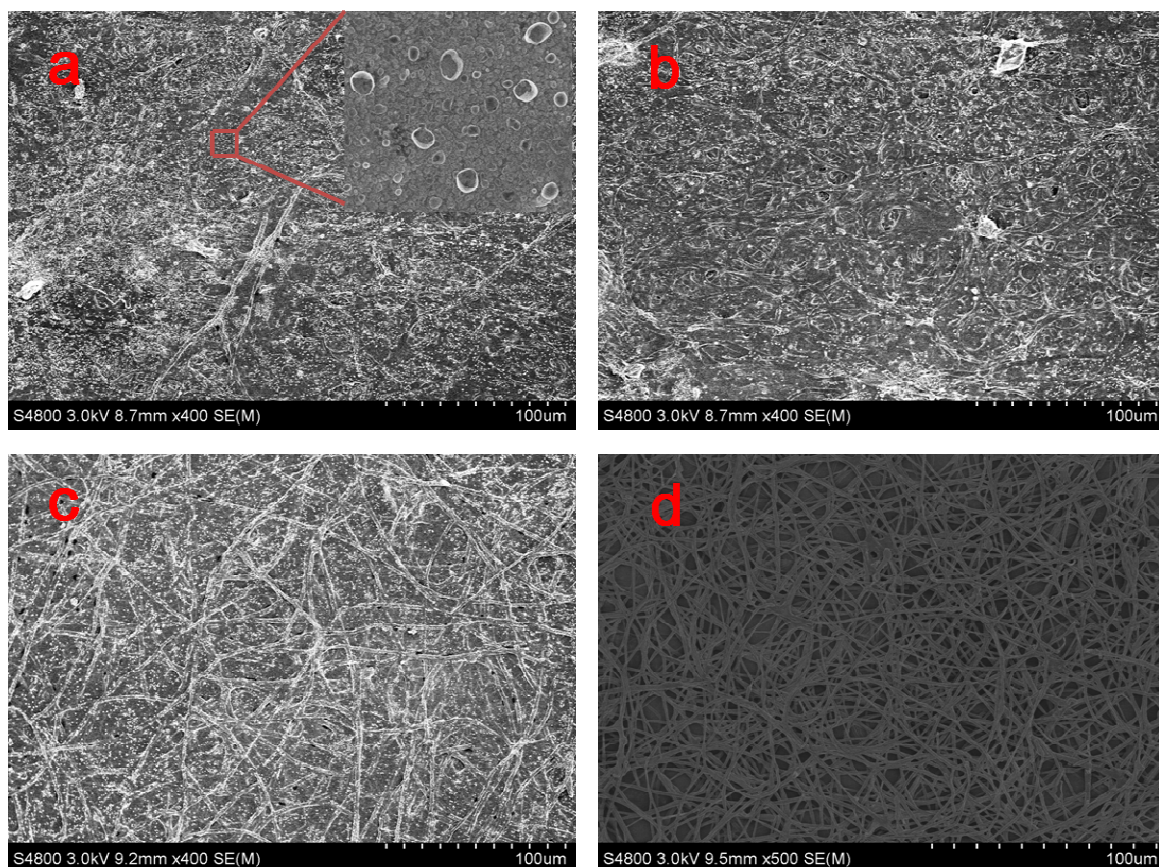


Figure S24. SEM images of spherical vesicles gradually converted to microtubes during the self-assembly process: (a) two weeks; (b) a month; (c) two months; (d) four months.

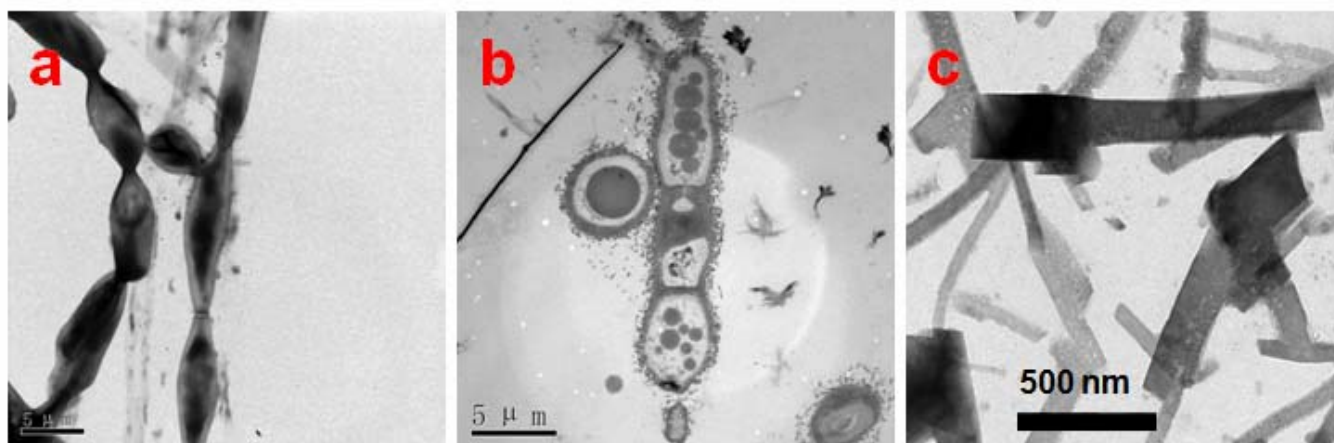


Figure S25. TEM images of necklace-like structures (a and b) and sheet-like structures (c).

8. Application of the microtubes of **1** in the adsorption of TNT

The peak at around 230 nm was attributed to the absorbance of TNT while the peak at around 290 nm was attributed to the absorbance of free **1** and **4**. A decrease in the characteristic absorbance of TNT from 0.342 to 0.065 after the microtubes of **1** were immersed into an aqueous solution of TNT (2.0×10^{-4} mg/mL) confirmed that TNT was adsorbed by microtubes (Figure S26, spectra a and d). Furthermore, this characteristic absorbance did not decrease after free **1** or **4** was added into this aqueous solution (Figure S26, spectra a, b, and c).

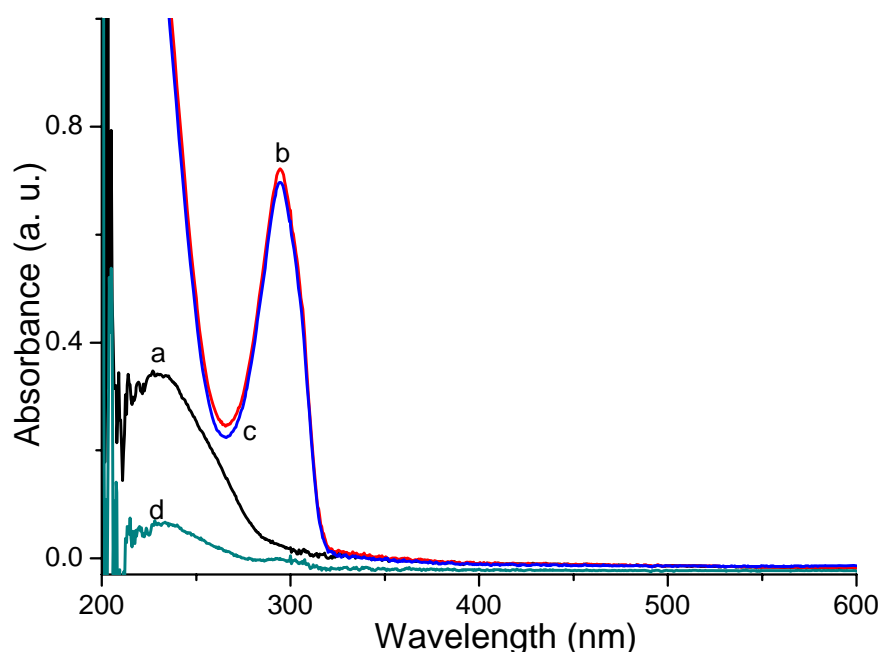
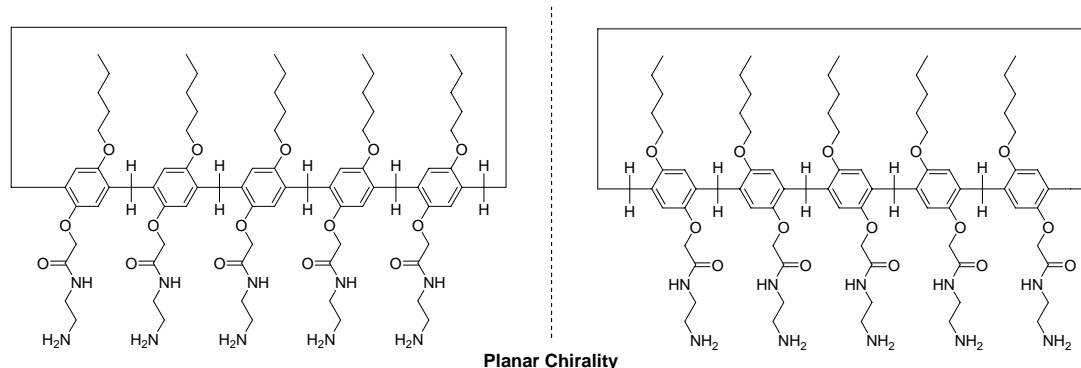


Figure S26. The UV-vis spectra: (a) TNT; (b) **1** and TNT; (c) **4** and TNT; (d) after microtubes of **1** were immersed into the aqueous solution of TNT. These experiments demonstrated that TNT can be efficiently removed by simple filtration after the microtubes of **1** were immersed into the TNT aqueous solution.

9. Another advantage of macrocyclic amphiphiles

The cyclic structure of **1** can provide an enantiomeric pair of **1** based on planar chirality,^{S4} not constitutional isomers, according to the relative orientation of the substituents as shown below.



In this communication, we used **1** as a racemic mixture. The enantiomeric pair of **1** could not be separated, possibly because flipflop of the aryl moieties is too fast. Actually compound **2a**, the precursor of **1**, is also a racemic mixture as shown by its crystal structure (Figure S27). However, if block substituents are introduced,^{S4} the enantiomeric pair of **1** will possibly become optically isolated and each enantiomer may show different self-assembly behaviors with different functions. This can be another advantage of macrocyclic amphiphiles.

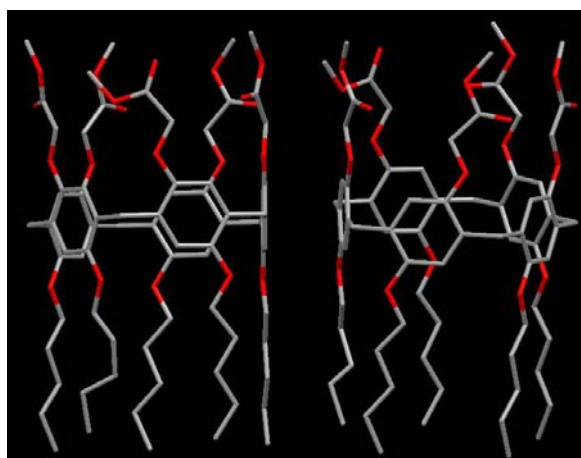


Figure S27. A view of the crystal structure of **2a** showing that it contains an enantiomeric pair based on planar chirality in the solid state.

References:

- S1. Yao, Y.; Xue, M.; Chi, X.; Ma, Y.; He, J.; Abliz, Z.; Huang, F. *Chem. Commun.* **2012**, 48, 6505–6507.
- S2. Ogoshi, T.; Kanai, S.; Fujinami, S.; Yamagishi, T. A.; Nakamoto, Y. *J. Am. Chem. Soc.* **2008**, 130, 5022–5023.
- S3. Lee, M.; Lee, S.-J.; Jiang, L.-H. *J. Am. Chem. Soc.* **2004**, 126, 12724–12725.
- S4. Ogoshi, T.; Masaki, K.; Shiga, R.; Kitajima, K.; Yamagishi, T.-a. *Org. Lett.* **2011**, 13, 1264–1266.